Spring 3-17-2017

Metal-containing polymers bearing pendant nickel(II) complexes of Goedken's macrocycle

Joseph A. Paquette

Amir Rabiee Kenaree

Joe Gilroy
jgilroy5@uwo.ca

Metal-containing polymers bearing pendant nickel(II) complexes of Goedken's macrocycle

Joseph A. Paquette, Amir Rabiee Kenaree and Joe B. Gilroy*

Department of Chemistry and the Centre for Advanced Materials and Biomaterials Research (CAMBR), The University of Western Ontario, 1151 Richmond St. N., London, Ontario, Canada, N6A 5B7. Tel: +1-519-661-2111 ext. 81561; E-mail: joe.gilroy@uwo.ca

TOC Graphic
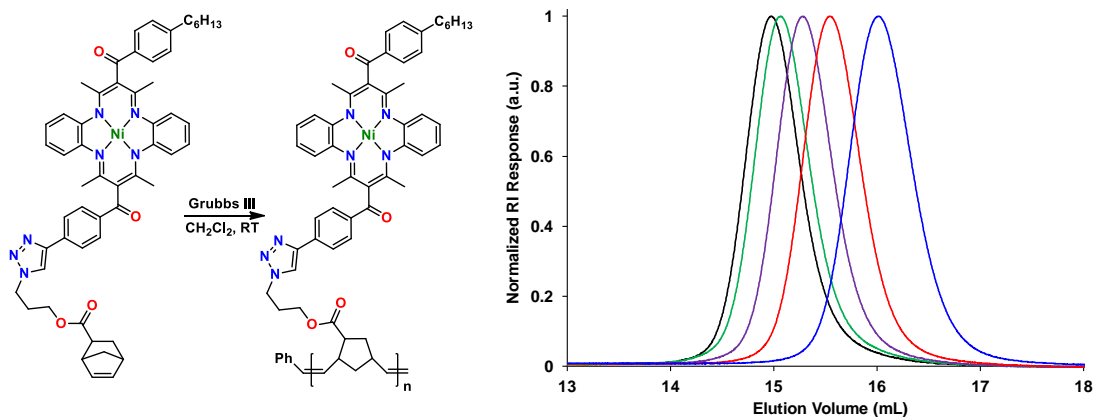
Abstract

The design, synthesis, and polymerization of a norbornene-based monomer bearing a nickel(II) complex of Goedken's macrocycle (**endo-13**) and the characterization of the resulting polymer are described. Detailed studies of the ring-opening metathesis polymerization of **endo-13** using the 3-bromopyridine adduct of Grubbs' 3rd generation catalyst revealed that the polymerization shares many characteristics associated with a living polymer, but deviated from ideal behavior when high degrees of polymerization were targeted. The installation of a 3-hexylphenyl substituent at the macrocyclic backbone allowed for the realization of soluble polymers (**14**) and shut down an oxidative dimerization pathway commonly associated with metal complexes of Goedken's macrocycle. The cyclic voltammogram of the polymer **14** was comprised of two one-electron oxidation waves (0.21 V and 0.70 V relative to ferrocene/ferrocenium) associated with the stepwise oxidation of the macrocyclic ligand backbone and a one electron reduction wave associated with the reduction of nickel(II) to nickel(I) (−2.07 V). Solution and solid-state UV-vis absorption spectra recorded for polymer **14** revealed a strong $\pi \rightarrow \pi^*$ absorption (λ_{max} = 390 nm) and a ligand-to-metal charge transfer band (λ_{max} = 590 nm) typical of nickel(II) complexes of Goedken's macrocycle, and confirmed the absence of macrocycle-macrocycle interactions. This work has ultimately led to the development of a controlled polymerization route to a rare example of a side-chain nickel-containing polymer with potentially useful properties.

Introduction

Metal-containing polymers, or metallopolymers, have attracted significant attention due to their use as processable functional materials.[1-6] In the past decade, as a result of the development of polymerization methods with increasing functional group tolerance, polymers bearing group 8 and 9 transition metals in their pendant side chains (*e.g.*, **1–3**) have emerged as a promising subclass of metal-containing polymers.[7-18] These polymers have shown utility, for example, as the functional component of redox-active capsules,[19] as antimicrobial surfaces,[20] and as precursors to nanostructured materials.[21-23]
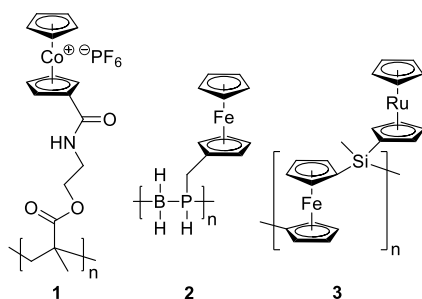
Nickel-containing polymers (*e.g.*, **4–7**)[24-28] remain relatively scarce throughout the literature when compared to polymers based on first row metals such as iron and cobalt. There are two primary reasons behind this scarcity. Firstly, the square planar ligand fields generally associated with nickel(II) complexes encourage π-stacking interactions, rendering most complexes poorly suited for polymerization studies as the targeted materials would likely have poor solubilities. Second, relatively few nickel(II) complexes exist that exhibit the stability required to tolerate most polymerization reactions and that also possess synthetic handles allowing for the introduction of polymerizable groups.

Ar = bis-2,5-(nonoxy)phenyl

4

5

Ar = 9,9-dioctylfluorene

6

7
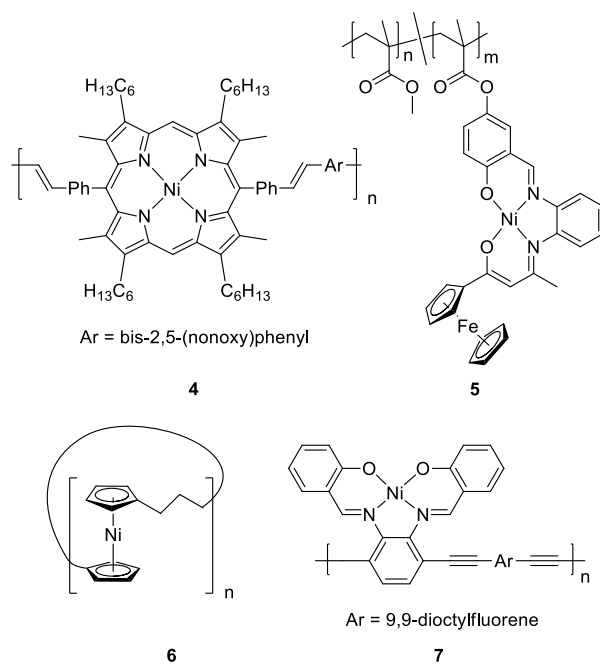
The stable, soluble nickel(II) complex of 4,11-dihydro-5,7,12,14-tetramethyldibenzo[b,i]-[1,4,8,11]tetraazacyclotetradecine (*i.e.*, Geodken's macrocycle) **8** can be produced in a single step in large quantities (> 10 g) and high yield (*ca.* 90%) from inexpensive starting materials,[29-30] and exhibits unusual ligand-centred redox chemistry (Fig. 1).[31] Furthermore, the macrocyclic backbone can be benzoylated at the activated α carbons, providing a synthetic handle for the introduction of polymerizable groups and preventing oxidative dimerization.[32-34]
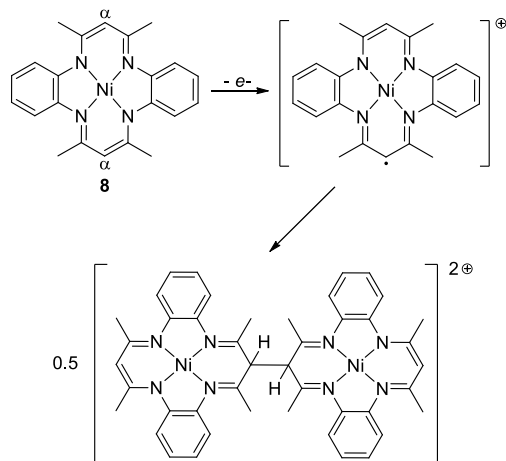
**Fig. 1** Oxidative dimerization of complex **8**.

Although derivatives of complex **8** have garnered significant interest from inorganic chemists for over five decades,[35-41] very little has been reported with respect to their incorporation into polymers. Prior to our recent work on main-chain polymers,[33-34] the only existing examples were produced in small quantities by electropolymerization.[31, 42-43] A polymer-substituted derivative of complex **8** has also been used to template ladder-like nanostructures.[44] Herein, we report the design, synthesis, and characterization of side-chain metal-containing polymers produced by ring-opening metathesis polymerization (ROMP) of functionalized nickel(II) complexes of Goedken's macrocycle in an effort to expand the scope of nickel-containing polymer chemistry.

Results and discussion

Monomer synthesis

The synthesis of the monomer used in this study (Scheme 1) began with the reaction of 4-hexylbenzoyl chloride with macrocycle **8** in the presence of Et$_3$N to afford complex **9** in 21% yield. The reaction mixture also contained complex **8** (26%) and the di-4-*n*-hexylbenzoyl

5

substituted macrocycle (28%). For the purposes of this study, the 4-hexylbenzoyl substituent was chosen to increase the solubility of the target polymers and to circumvent potential chemical and redox reactivity at the α C-H groups present on the ligand backbone of complex **8** and its analogs. Next, 4-(trimethylsilylethynyl)benzoyl chloride was combined with **9** in the presence of Et$_3$N to afford compound **10** in 91% yield. The ethynyl group was deprotected using K$_2$CO$_3$ to afford compound **11** in 85% yield. Compound ***endo*-12** was synthesized in 89% yield, by combining 3-azido-1-propanol with *endo*-5-norbornene-2-carboxylic acid, using the Steglich esterification.[45] We chose to employ the *endo*-norbornene derivative, which was produced according to an existing protocol,[46] because it afforded the advantages of simplified ^{1}H and ^{13}C{^{1}H} NMR spectra and reduced reaction rates[47] allowing us to study the subsequent polymerization reactions in detail. Finally, the copper-assisted azide-alkyne cycloaddition (CuAAC) reaction between **11** and ***endo*-12** gave the monomer (***endo*-13**) in 54% yield. Each of the molecular species described were characterized by high-resolution mass spectrometry, ^{1}H and ^{13}C{^{1}H} NMR spectroscopy, FT-IR and UV-vis absorption spectroscopy (Fig. S1–S10).
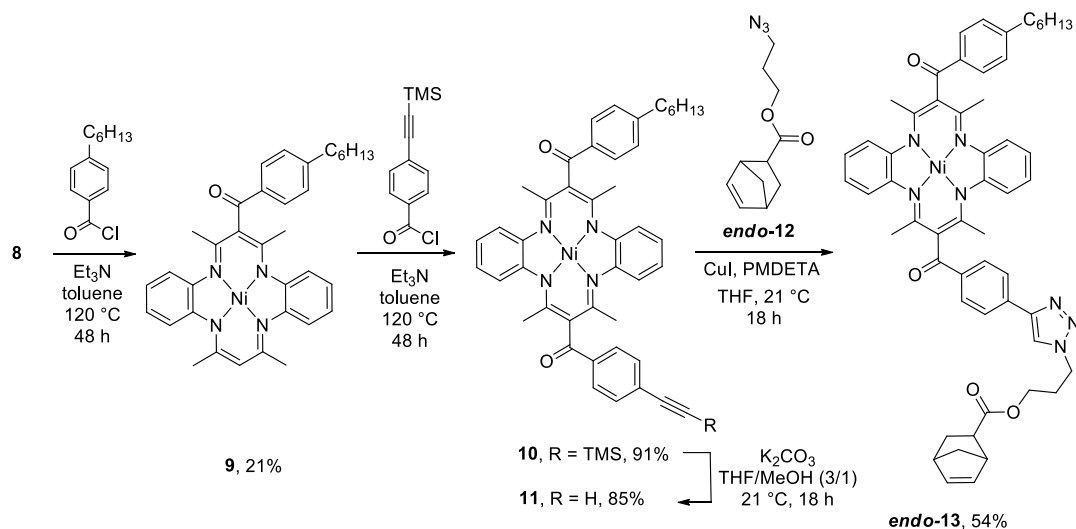
Scheme 1   Synthesis of monomer ***endo*-13**.

Polymerization studies

      ROMP was chosen for this study due to its functional group tolerance. Solvent choice can affect ROMP reactions,[48] therefore, we began our polymerization studies by probing reactions in different solvents. A typical polymerization reaction involved the rapid introduction of a solution of the 3-bromopyridine derivative of Grubbs' 3rd generation catalyst (Grubbs III) to a stirring solution of **endo-13** at room temperature (21 °C) with a monomer-to-catalyst ratio of 50:1 (Scheme 2). Reactions were performed in THF, DMF, and CH_2Cl_2 and the resulting polymers were analyzed by gel permeation chromatography (GPC). The polymer produced in THF had a broad molecular weight distribution ($Đ = 2.69$) and the reaction did not proceed when performed in DMF. The polymerization in CH_2Cl_2 produced polymers with narrow molecular weight distributions ($Đ = 1.12$), typical of a controlled polymerization protocol such as ROMP.
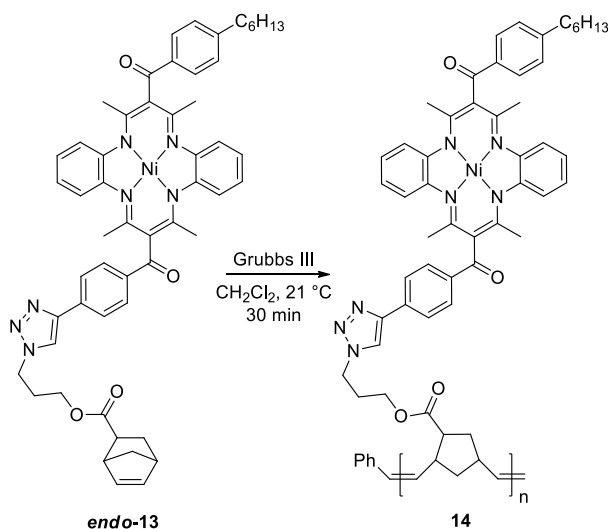
Scheme 2   ROMP of monomer **endo-13**.

Table 1   Molecular weight data for samples of polymer **14** produced in different solvents.

Solvent	M_n (g mol^{-1})^a	M_w (g mol^{-1})^a	$Đ^a$
THF	16,500	44,600	2.69
DMF^b	-	-	-
CH$_2$Cl$_2$	24,100	26,500	1.12

^{a}Conventional calibration GPC relative to polystyrene standards. ^{b}No polymer produced.

The polymerization of monomer ***endo*-13**, in CH$_2$Cl$_2$, was confirmed by the disappearance of signals associated with norbornene in the monomer (6.24 and 5.96 ppm) and appearance of olefinic signals associated with the polymer backbone (5.63−5.06 ppm) in the corresponding ^{1}H NMR spectra of aliquots taken from the reaction mixture (Fig. S11). The reactions neared completion after approximately 15 min, and were stirred for an additional 15 min to ensure complete consumption of monomer. Ethyl vinyl ether (EVE) was then added to poison the catalyst and terminate polymerization. The reaction mixtures were passed through a neutral alumina plug using THF as eluent to remove the catalyst. Precipitation from THF into Et$_2$O followed by centrifugation and drying *in vacuo* afforded polymer **14** in greater than 80% yield.

In order to further investigate the polymerization behaviour of ***endo*-13**, we performed two different studies. Often, the molecular weight of polymers produced by ROMP can be determined by ^{1}H NMR end-group analysis. In our specific case, the signals associated with the phenyl end group were shrouded by the aromatic proton signals associated with Goedken's macrocycle. Therefore, the molecular weights of the polymers produced during these studies were estimated using GPC analysis. The first study involved monitoring a single ROMP reaction (monomer:catalyst 50:1) as a function of time (Fig. 2a). The molecular weight of the isolated polymers increased over time, with the reaction nearing completion around 600 s before the molecular weight plateaued as a sign of the completion of the reaction. This behaviour was

consistent with a well-behaved ROMP reaction, whereby the rate of reaction decreases as the monomer is consumed. The consumption of monomer as a function of time was also monitored by ^{1}H NMR spectroscopy using integration data to establish the ratio of olefinic protons associated with *endo*-**13** and polymer **14**. The controlled nature of the polymerization was also confirmed by the observation of a linear behavior when $\ln([M]_o/[M])$ was plotted *vs.* time (semilogarithmic plot), where $[M]_0$ was the initial concentration of monomer and $[M]$ was the concentration of monomer at different time intervals (Fig. 2b).
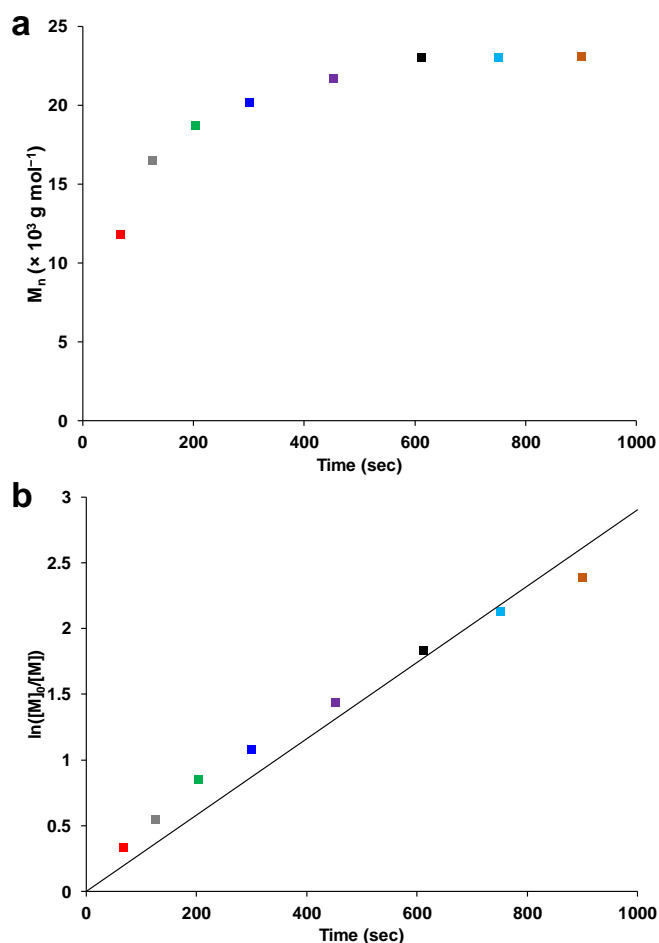
Fig. 2 (a) Number average molecular weight (M_n, GPC) of polymer **14** as a function of time. (b) Semilogarithmic plot for the consumption of monomer *endo*-**13** as a function of time. $[M]_0/[M]$ was determined using integration data from ^{1}H NMR spectroscopy. The best fit trendline is shown in black.

The second experiment was designed to further examine the ROMP of *endo-***13** and involved the variation of feed molar ratios (*i.e.*, monomer:catalyst ratios: 20, 40, 60, 80, and 100). The molecular weights, and thus the degrees of polymerization, were once again determined by GPC. The measured molecular weights of the polymers increased as the feed ratios were increased (Fig. 3). However, the trend deviated from ideal (black line) behavior in two ways. First, the molecular weights determined were lower than expected for each molar feed ratio. Careful analysis of the crude reaction mixtures confirmed that the monomer had been consumed in each case, ruling out incomplete monomer conversion as a potential explanation for this behavior. Rather, we attribute this behavior to the poor structural match between polymer **14** and the monodisperse polystyrene standards employed during the conventional calibration GPC experiments. Second, the linear relationship between monomer:catalyst ratio and DP_n expected was not maintained at high feed molar ratios, indicating that side reactions and/or quenching occurs when the number of propagation steps are increased. The dispersity values calculated for the polymers also increased gradually with increasing feed molar ratio, corroborating this conclusion. Combining the results of our polymerization studies allowed for the conclusion that the ROMP of *endo-***13** is well-behaved, although it cannot be formally classified as living.
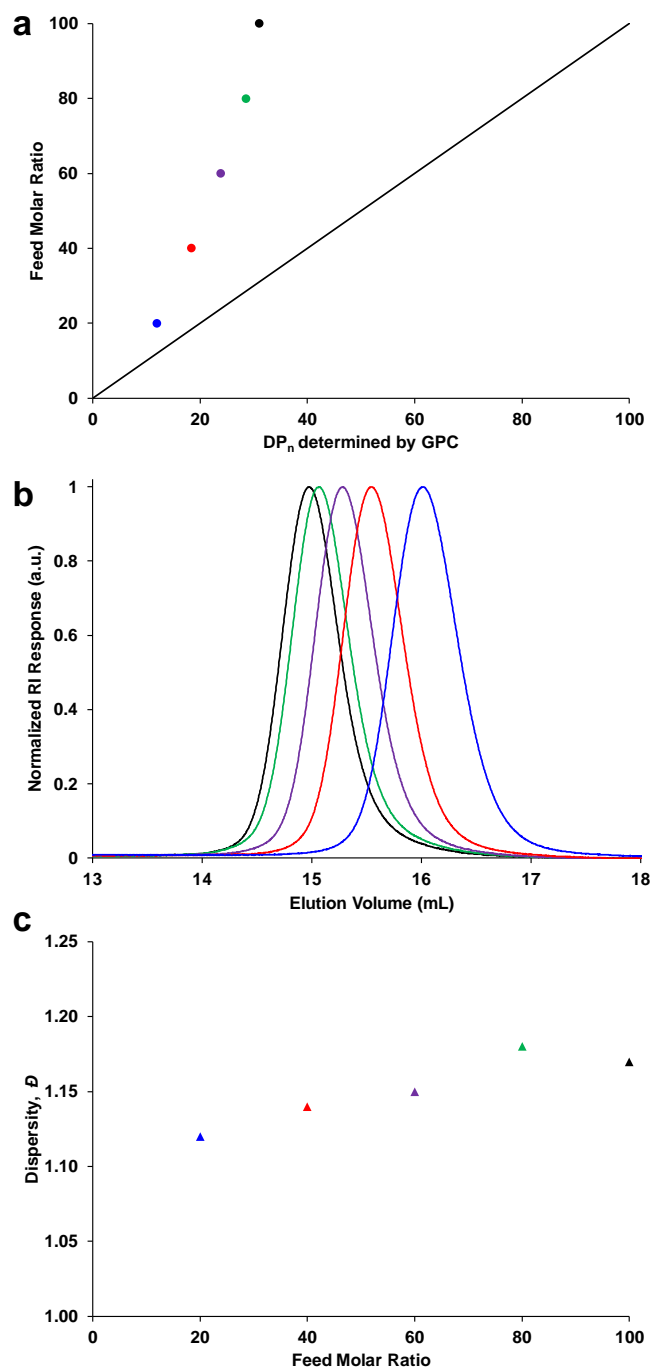
Fig. 3 (a) Relationship of feed molar ratio and DP_n determined by GPC. The black line depicts ideal behaviour. (b) GPC traces for samples of polymer **14** prepared at different feed molar ratios. (c) Dispersity of samples of polymer **14** prepared at different feed molar ratios.

Polymer characterization

Thermal gravimetric analysis of a representative sample of polymer **14** revealed its stability up to 278 °C, followed by a rapid decomposition to *ca.* 40% mass, and slow decomposition to an overall char yield of 6% when the temperature reached 1000 °C (Fig. S12). A sample of polymer **14** was also analyzed by differential scanning calorimetry between −50 °C and 250 °C, revealing a glass transition temperature of 211 °C (Fig. S13).

The UV-vis absorption spectra recorded in CH_2Cl_2 for ***endo*-13** and polymer **14** were essentially identical (Fig. 4a). The characteristic absorption maxima for nickel(II) complexes of Goedken's macrocycle centred at λ_{max} 390 nm ($\pi \rightarrow \pi^*$) and λ_{max} 590 nm (LMCT)[49] were present in both spectra, confirming that the electronic structure of the macrocycle was unaltered upon polymerization. The thin-film absorption properties of polymer **14** were also studied (Fig. 4b). The striking similarities between the solution and thin-film spectra of polymer **14** indicated a lack of significant intermolecular interactions (*e.g.*, π-π stacking) between polymer-bound macrocycle units in the solid state.
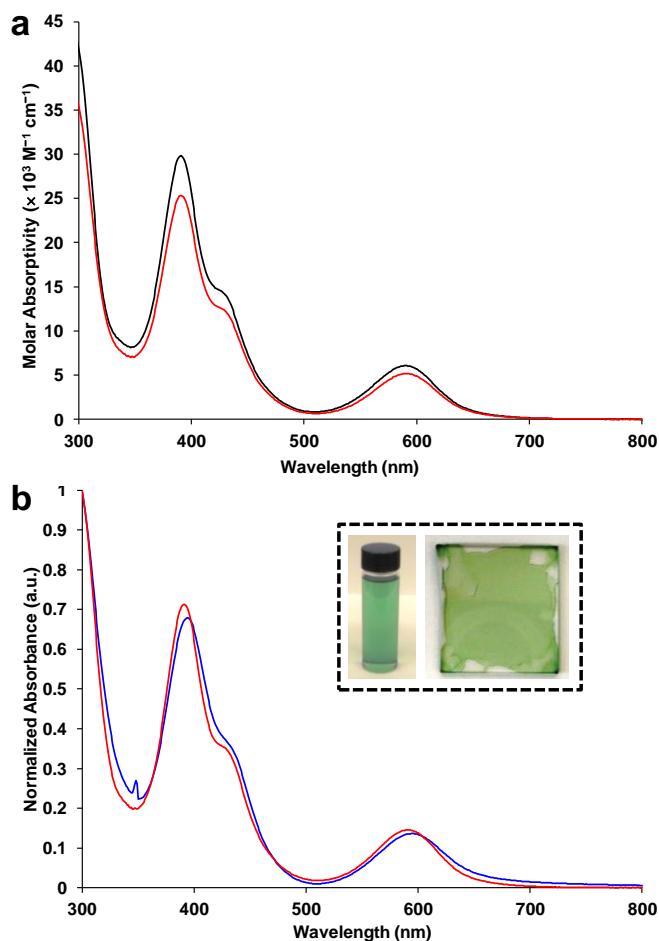
Fig. 4 (a) UV-vis absorption spectra monomer *endo*-**13** (black) and polymer **14** (red) recorded in CH_2Cl_2. (b) Normalized UV-vis absorption spectra of polymer **14** in CH_2Cl_2 (red) and as a thin film (blue). Pictures of polymer **14** as a 10^{-4} M (with respect to repeating unit) CH_2Cl_2 solution and thin film are shown in the inset of panel (b).

The electrochemical properties of monomer *endo*-**13** and polymer **14** were investigated using cyclic voltammetry in CH_2Cl_2 (Fig. 5, Table 2). The voltammogram of *endo*-**13** included two reversible oxidation waves at E°_{ox1} = 0.21 and E°_{ox2} = 0.72 V, relative to the ferrocene/ferrocenium redox couple. These waves correspond to the stepwise, ligand-centred oxidation of the nickel(II) complex of Goedken's macrocycle (NiL) to the radical cation (NiL → NiL$^{\bullet+}$) followed by oxidation to the dication (NiL$^{\bullet+}$ → NiL^{2+}). Crucially, through judicious

monomer design, we have shut down the oxidative dimerization pathway commonly associated with nickel(II) complexes of Goedken's macrocycle, as evidenced by the reversibility of the oxidation waves. An irreversible reduction was also observed for the monomer at a cathodic potential of −2.14 V, which has been previously attributed to the reduction of nickel(II).[32] The voltammogram of polymer **14** was quite similar. In CH_2Cl_2, the first oxidation was reversible and centred at $E°_{ox1} = 0.21$. The second oxidation wave was irreversible due to plating of the poly dication onto the working electrode surface, with an anodic peak potential of 0.70 V. Unfortunately, the degree of diffusion control associated with our experiments was not improved when THF and CH_2Cl_2/THF solvents were employed (Fig. S14). Furthermore, the polymer exhibited a reversible one-electron reduction wave associated with nickel(II),[32, 50] at $E°_{red1} = $ −2.07 V, potentially indicating that the macromolecular nature of the polymer protects the metal centre, and prevents side reactions and/or metal expulsion from occurring.
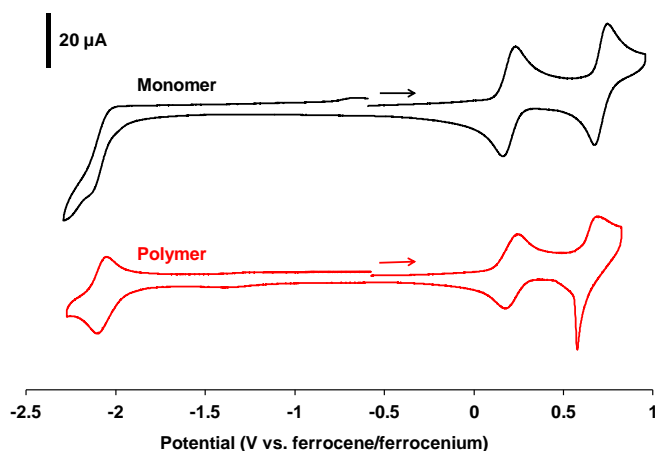
Fig. 5 Cyclic voltammograms of monomer ***endo*-13** (black) and polymer **14** (red) recorded at a scan rate of 250 mV s^{-1} in CH_2Cl_2 solutions containing 1×10^{-3} M analyte and 0.1 M [nBu$_4$N][PF$_6$] as supporting electrolyte.

Table 2   Cyclic voltammetry data for monomer *endo*-**13** and polymer **14**.

Compound	E°_{red1}	E°_{ox1}	E°_{ox2}
endo-**13**	-2.14^{a}	0.21	0.72
14	-2.07	0.21	0.70^{a}

[a]Irreversible process, potential at maximum cathodic/anodic peak current quoted.

Conclusions

Through the careful design of monomer *endo*-**13**, which incorporated a norbornene group suitable for ROMP, a rare example of a side-chain nickel-containing polymer **14** was realized. Detailed studies of the ROMP reaction catalyzed by the 3-bromopyridine derivative of Grubbs' 3rd generation catalyst were performed, revealing many characteristics associated with a living polymerization. When greater degrees of polymerization were targeted, small deviations from ideal living behavior, likely relating to premature termination, were noted. UV-vis absorption spectroscopy showed that polymer **14** maintained the electronic structure associated with the nickel(II) complexes of Goedken's macrocycle in solution and the solid state, confirming the absence of macrocycle-based intra- or intermolecular interactions. Cyclic voltammetry studies led us to similar conclusions, whereby both monomer and polymer exhibited two reversible one-electron oxidation waves associated with Goedken's macrocycle. A reversible one-electron reduction was also observed for the polymer. Our future work in this area will involve further development of metal complexes of *N*-donor ligands, including Goedken's macrocycle, amenable to ROMP and other controlled polymerization methods.

Experimental section

General considerations

Reactions and manipulations were carried out under a nitrogen atmosphere using standard Schlenk or glove box techniques unless otherwise stated. Solvents were obtained from Caledon

Laboratories, dried using an Innovative Technologies Inc. solvent purification system, collected under vacuum, and stored under a nitrogen atmosphere over 4 Å molecular sieves. Reagents were purchased from Sigma-Aldrich, Alfa Aesar, or Oakwood Chemical and used as received unless otherwise stated. 4-[(trimethylsilyl)ethynyl]-benzoyl chloride,[51] compound **8**,[30] 3-azido-1-propanol[52] and *endo*-5-norbornene-2-carboxylic acid[46] were prepared according to published protocols. NMR spectra were recorded on a 600 MHz (^{1}H: 599.3 MHz, ^{13}C{^{1}H}: 150.7 MHz) Varian INOVA instrument or a 400 MHz (^{1}H 400.1 MHz, ^{13}C{^{1}H}: 100.6 MHz) Varian Mercury instrument. ^{1}H NMR spectra were referenced to residual CHCl$_3$ (7.27 ppm) and ^{13}C{^{1}H} NMR spectra were referenced to CDCl$_3$ (77.0 ppm). Mass spectrometry data were recorded in positive-ion mode with a Bruker microTOF II instrument using electrospray ionization. UV-vis absorption spectra were recorded for CH$_2$Cl$_2$ solutions and thin films using a Cary 5000 spectrophotometer. Four separate concentrations were run for each sample and molar extinction coefficients were determined from the slope of a plot of absorbance against concentration. Thin films were produced by spin coating a chlorobenzene solution of the polymer (15 mg mL^{-1}) on a glass slide, at 3000 rpm. FT-IR spectra were recorded on a PerkinElmer Spectrum Two instrument using an attenuated total reflectance accessory or as KBr pellets using a Bruker Vector 33 FT-IR spectrometer.

Gel permeation chromatography

GPC experiments were conducted in chromatography-grade THF at concentrations of 5 mg mL^{-1} using a Viscotek GPCmax VE 2001 GPC instrument equipped with an Agilent PolyPore guard column (PL1113-1500) and two sequential Agilent PolyPore GPC columns packed with porous poly(styrene-*co*-divinylbenzene) particles (MW range: 200–2,000,000 g mol^{-1}; PL1113-6500) regulated at a temperature of 30 °C. Signal responses were measured using a Viscotek VE 3580

RI detector, and molecular weights were determined by comparison of the maximum RI response with a calibration curve (10 points, 1,500–786,000 g mol^{-1}) established using monodisperse polystyrene standards purchased from Viscotek.

Thermal analysis

Thermal degradation studies were performed using a TA Instruments Q50 TGA. Samples were placed in a platinum pan and heated at a rate of 10 °C min^{-1} from 35 to 1000 °C under a flow of nitrogen (60 mL min^{-1}). Differential scanning calorimetry (DSC) thermograms were acquired using a TA Instruments DSC Q20 instrument. The polymer samples were placed in an aluminum Tzero pan and heated from room temperature to 250 °C at 10 °C min^{-1} under a flow of nitrogen (50 mL min^{-1}) and cooled down to −50 °C at 10 °C min^{-1}, before they underwent two additional heating/cooling cycles.

Electrochemical methods

Cyclic voltammetry experiments were performed with a Bioanalytical Systems Inc. (BASi) Epsilon potentiostat and analyzed using BASi Epsilon software. Typical electrochemical cells consisted of a three-electrode setup including a glassy carbon working electrode, platinum wire counter electrode, and silver wire *pseudo*-reference electrode. Experiments were run at a scan rate of 250 mV s^{-1} in dry and degassed CH_2Cl_2, THF, and THF/CH_2Cl_2 solutions of the analyte (~1 mM) and electrolyte (0.1 M [nBu$_4$N][PF$_6$]). Cyclic voltammograms were referenced against the ferrocene/ferrocenium redox couple (~1 mM internal standard) and corrected for internal cell resistance using the BASi Epsilon software.

Synthesis of 4-hexylphenyl substituted macrocycle 9

A Schlenk flask equipped with a stir bar was charged with complex **8** (10.0 g, 24.9 mmol), 4-hexylbenzoyl chloride (5.44 mL, 24.9 mmol) and dry toluene (250 mL). Dry and degassed Et$_3$N

(27.8 mL, 199 mmol) was added and the vessel was fitted with a condenser and heated to 125 °C. After stirring for 16 h, the mixture was cooled to room temperature, filtered, and the solvent was removed *in vacuo*. Column chromatography (CH_2Cl_2/toluene, 1:1, 350 mL silica gel, R_f = 0.17) was performed to yield complex **9** as a dark green microcrystalline solid. Yield = 3.02 g, 21%. In addition, 2.56 g (26%) of complex **8** and 5.41 g (28%) of the disubstituted analog were also isolated. ^{1}H NMR (400.1 MHz, CDCl$_3$): δ 8.13 (d, 2H, J_{HH} = 8 Hz, aryl C*H*), 7.34 (d, 2H, J_{HH} = 9 Hz, aryl C*H*), 6.72 (d, 2H, J_{HH} = 8 Hz, aryl C*H*) 6.65−6.58 (m, 4H, aryl C*H*), 6.56−6.53 (m, 2H, aryl C*H*), 4.86 (s, 1H, C*H*), 2.70 (t, 2H, J_{HH} = 8 Hz, C*H*$_2$), 2.10 (s, 6H, macrocycle C*H*$_3$), 1.91 (s, 6H, macrocycle C*H*$_3$), 1.70–1.63 (m, 2H, C*H*$_2$), 1.40–1.30 (m, 6H, C*H*$_2$), 0.90 (t, 3H, C*H*$_3$). ^{13}C{^{1}H} NMR (150.7 MHz, CDCl$_3$) δ 200.1, 155.3, 153.7, 149.2, 147.4, 147.3, 136.9, 129.9, 128.9, 122.7, 121.8, 121.7, 121.1, 120.8, 111.2, 36.1, 31.7, 31.1, 29.0, 22.6, 21.9, 20.6, 14.1. FT-IR (ATR): 2964 (w), 2923 (w), 2853 (w), 1653 (w), 1602 (w), 1530 (m), 1453 (m), 1430 (m), 1380 (s), 1260 (m), 1215 (m), 1171 (m), 1020 (m), 914 (m), 799 (m), 742 (s), 583 (w), 535 (w). UV-vis (CH$_2$Cl$_2$): λ_{max} (ε) 588 nm (5,800 M^{-1} cm^{-1}), 434 nm (sh, 12,200 M^{-1} cm^{-1}), 393 nm (32,800 M^{-1} cm^{-1}), 269 nm (44,000 M^{-1} cm^{-1}). Mass Spec. (EI, +ve mode) *m/z*: [M]$^+$ calc'd for [C$_{35}$H$_{38}$N$_4$NiO]$^+$, 588.2399; found, 588.2387; difference: −2.0 ppm.

Synthesis of asymmetrically substituted macrocycle 10

A Schlenk flask equipped with a stir bar was charged with complex **9** (0.45 g, 0.76 mmol), 4-[(trimethylsilyl)ethynyl]benzoyl chloride (0.22 g, 0.92 mmol) and dry toluene (45 mL). Dry and degassed Et$_3$N (0.85 mL, 6.1 mmol) was added and the vessel was fitted with a condenser and heated to 125 °C under a N$_2$ atmosphere. After stirring for 16 h, the mixture was cooled to room temperature, filtered, and the solvent was removed *in vacuo*. Column chromatography (CH$_2$Cl$_2$/toluene, 2:1, 750 mL silica gel, R_f = 0.12) was performed to yield complex **10** as a dark

green solid. Yield = 0.55 g, 91%. ^{1}H NMR (599.3 MHz, CDCl$_3$): δ 8.22–8.11 (m, 4H, aryl C*H*), 7.66 (d, 2H, J_{HH} = 8 Hz, aryl C*H*), 7.38 (d, 2H, J_{HH} = 8 Hz, aryl C*H*), 6.68–6.62 (m, 4H, aryl C*H*), 6.62–6.56 (m, 4H, aryl C*H*), 2.72 (t, 2H, J_{HH} = 8 Hz, C*H*$_2$), 1.92 (s, 6H, macrocycle C*H*$_3$), 1.90 (s, 6H, macrocycle C*H*$_3$), 1.72–1.64 (m, 2H, C*H*$_2$), 1.43–1.29 (m, 6H, C*H*$_2$), 0.90 (t, 3H, C*H*$_3$), 0.29 (s, 9H, SiC*H*$_3$). ^{13}C{^{1}H} NMR (150.7 MHz, CDCl$_3$) δ 200.0, 199.5, 153.7, 153.7, 149.3, 147.3, 147.2, 138.5, 136.7, 132.5, 129.9, 129.5, 129.0, 128.2, 122.8, 122.6, 121.8, 121.4, 120.8, 104.2, 98.4, 36.1, 31.6, 31.1, 29.0, 22.6, 20.4, 20.4, 14.1, –0.2. FT-IR (ATR): 3064 (w), 2924 (w), 2854 (w), 1652 (m), 1598 (m), 1491 (m), 1449 (m), 1429 (m), 1362 (s), 1323 (m), 1222 (s), 1169 (m), 1053 (m), 919 (m), 841 (s), 743 (s) cm^{-1}. UV-vis (CH$_2$Cl$_2$): λ$_{max}$ (ε) 590 nm (6,000 M^{-1} cm^{-1}), 430 nm (sh, 14,200 M^{-1} cm^{-1}), 390 nm (30,200 M^{-1} cm^{-1}), 275 nm (60,500 M^{-1} cm^{-1}). Mass Spec. (ESI, +ve mode) *m/z*: [M]$^+$ calc'd for [C$_{47}$H$_{50}$N$_4$NiO$_2$Si]$^+$, 788.3056; found, 788.3059; difference: +0.4 ppm.

Synthesis of asymmetrically substituted macrocycle 11

Compound **10** (0.40 g, 0.51 mmol) was stirred with K$_2$CO$_3$ (0.14 g, 1.0 mmol) in THF/MeOH (3:1, 20 mL) for 16 h at room temperature. CH$_2$Cl$_2$ (50 mL) was then added and the organic layer was washed with 0.5 M aqueous NH$_4$Cl (50 mL), dried with MgSO$_4$ and concentrated *in vacuo*. The resulting dark green solid was purified via precipitation from a saturated CH$_2$Cl$_2$ solution in pentane to afford **11** as a dark green microcrystalline solid. Yield = 0.31 g, 85%. ^{1}H NMR (599.3 MHz, CDCl$_3$): δ 8.22 (d, 2H, J_{HH} = 7 Hz, aryl C*H*), 8.15 (s, 2H, aryl C*H*), 7.70 (d, 2H, J_{HH} = 8 Hz, aryl C*H*), 7.38 (d, 2H, J_{HH} = 8 Hz, aryl C*H*), 6.69–6.64 (m, 4H, aryl C*H*), 6.62–6.57 (m, 4H, aryl C*H*), 3.30 (s, 1H, alkyne C*H*), 2.72 (t, 2H, J_{HH} = 8 Hz, C*H*$_2$), 1.92 (s, 6H, macrocycle C*H*$_3$), 1.91 (s, 6H, macrocycle C*H*$_3$), 1.73–1.64 (m, 2H, C*H*$_2$), 1.42–1.30 (m, 6H, C*H*$_2$), 0.90 (t, 3H, C*H*$_3$). ^{13}C{^{1}H} NMR (150.7 MHz, CDCl$_3$) δ 200.1, 199.5, 153.8, 153.7, 149.4, 147.4, 147.2,

139.0, 136.7, 132.7, 129.9, 129.6, 129.0, 127.2, 122.8, 122.6, 121.8, 121.4, 120.8, 82.9, 80.6, 36.1, 31.7, 31.1, 29.0, 22.6, 20.5, 20.4, 14.1. FT-IR (ATR): 3291, 2923, 2853, 1657, 1600 (w), 1491 (w), 1530 (s), 1448 (m), 1428 (m), 1363 (s), 1323 (m), 1223 (s), 1170 (m), 1054 (m), 912 (m), 854 (m), 745 (s) cm^{-1}. UV-vis (CH_2Cl_2): λ_{max} (ε) 590 nm (5,700 M^{-1} cm^{-1}), 429 nm (sh, 13,400 M^{-1} cm^{-1}), 390 nm (28,500 M^{-1} cm^{-1}), 274 nm (62,300 M^{-1} cm^{-1}). Mass Spec. (ESI, +ve mode) *m/z*: $[M]^+$ calc'd for $[C_{44}H_{42}N_4NiO_2]^+$, 716.2661; found, 716.2658; difference: −0.4 ppm.

Synthesis of 3-azidopropyl *endo*-2-norbornene-2-carboxylate *endo*-12

Endo-5-norbornene-2-carboxylic acid (0.36 g, 2.6 mmol), dicyclohexylcarbodiimide (0.65 g, 3.2 mmol), and 4-(dimethylamino)pyridine (0.38 g, 3.1 mmol) were combined in dry/degassed CH_2Cl_2 (10 mL) and stirred for 15 min. The flask was then charged with a solution of 3-azido-1-propanol (0.29 g, 2.9 mmol in 5 mL CH_2Cl_2) and the resulting mixture stirred for an additional 1.5 h before the precipitate was removed via gravity filtration and the filtrate was concentrated *in vacuo*. Column chromatography (125 mL, silica gel, hexanes/Et_2O: 4/1, R_f = 0.33) was performed to yield ***endo*-12** as a colourless oil. Yield = 0.51 g, 89%. ^{1}H NMR (599.3 MHz, CDCl$_3$): δ 6.20 (dd, 1H, J_{HH} = 6, J_{HH} = 3 Hz, C=C*H*), 5.92 (dd, 1H, J_{HH} = 6, J_{HH} = 3 Hz, C=C*H*), 4.11 (t, 2H, J_{HH} = 6 Hz, C*H*$_2$), 3.38 (t, 2H, J_{HH} = 7 Hz, C*H*$_2$), 3.20 (s, 1H, C*H*), 2.98–2.93 (m, 1H, C*H*), 2.91 (s, 1H, C*H*), 1.94–1.85 {m, 3H, C*H*$_2$ (2H) and diastereotopic C*H*$_2$ (1H)}, 1.46–1.39 (m, 2H, 2 × diastereotopic C*H*$_2$), 1.28 (d, 1H, J_{HH} = 8 Hz, diastereotopic C*H*$_2$). ^{13}C{^{1}H} NMR (150.7 MHz, CDCl$_3$) δ 174.5, 137.8, 132.2, 61.0, 49.6, 48.2, 45.7, 43.3, 42.5, 29.2, 28.2. FT-IR (ATR): 3062 (w), 2969 (w), 2878 (w), 2095 (s), 1729 (s), 1455 (w), 1336 (m), 1270 (m), 1172 (s), 1132 (m), 1066 (m), 991 (w), 905 (w), 838 (w) 710 (s) cm^{-1}. Mass Spec. (ESI, +ve mode) *m/z*: $[M]^+$ calc'd for $[C_{11}H_{15}N_3O_2]^+$, 221.1164; found, 221.1158; difference: −2.7 ppm.

Synthesis of monomer *endo*-13

An oven-dried Schlenk flask was charged with CuI (1.3 mg, 0.068 mmol) and *N,N,N',N'',N''*-pentamethyldiethylenetriamine (15 μL, 0.068 mmol) in dry/degassed THF (50 mL) and stirred for 10 min. To the reaction mixture was added compounds **11** (1.00 g, 1.40 mmol) and ***endo*-12** (0.31 g, 1.40 mmol) and the mixture was stirred for 18 h at room temperature. The solvent was then removed *in vacuo*. As the concentrate contained some unreacted **11** and ***endo*-12** in addition to ***endo*-13**, the monomer was purified by column chromatography (125 mL, silica gel). First, a 19/1 mixture of toluene/EtOAc removed ***endo*-12** (R_f = 0.58) and then **11** (R_f = 0.51). The eluent was then changed to a 4/1 mixture of toluene/EtOAc to isolate the monomer ***endo*-13** (R_f = 0.29) as a dark green solid. Yield = 0.64 g, 54%. ^{1}H NMR (599.3 MHz, CDCl$_3$): δ 8.32 (d, 2H, J_{HH} = 7 Hz, aryl CH), 8.17 (d, 2H, J_{HH} = 7 Hz, aryl CH), 8.06 (d, 2H, J_{HH} = 8 Hz, aryl C*H*), 7.94 (s, 1H, triazole-C*H*), 7.40 (d, 2H, J_{HH} = 8 Hz, aryl C*H*), 6.70–6.64 (m, 4H, aryl C*H*), 6.63−6.56 (m, 4H, aryl C*H*), 6.24 (dd, 1H, J_{HH} = 5, J_{HH} = 3 Hz, C=C*H*), 5.96 (dd, 1H, J_{HH} = 6, J_{HH} = 3 Hz, C=C*H*), 4.55 (t, 2H, J_{HH} = 6 Hz, C*H*$_2$), 4.18–4.10 (m, 2H, C*H*$_2$), 3.23 (s, 1H, C*H*), 3.02–2.96 (m, 1H, C*H*), 2.94 (s, 1H, C*H*), 2.73 (t, 2H, J_{HH} = 8 Hz, C*H*$_2$), 2.38–2.29 (m, 2H, C*H*$_2$), 1.95 (s, 6H, macrocycle C*H*$_3$), 1.93 (s, 6H, C*H*$_3$), 1.75–1.64 (m, 2H, C*H*$_2$), 1.51–1.21 (m, 10H, C*H*$_2$), 0.91 (t, 3H, C*H*$_3$). ^{13}C{^{1}H} NMR (150.7 MHz, CDCl$_3$) δ 200.0, 199.7, 174.5, 153.7, 153.6, 149.4, 147.3, 147.3, 146.8, 138.6, 138.0, 136.7, 135.3, 132.1, 130.4, 129.9, 129.0, 126.0, 122.7, 122.6, 121.8, 121.4, 121.0, 120.8, 60.5, 49.7, 47.4, 45.7, 43.3, 42.5, 36.1, 31.6, 31.1, 29.6, 29.2, 29.0, 22.5, 20.4, 20.4, 14.0. FT-IR (ATR): 3058 (w), 2928 (w), 2856 (w), 1729 (m), 1652 (m), 1603 (m), 1531 (s), 1448 (m), 1429 (m), 1363 (s), 1326 (m), 1224 (s), 1171 (s), 1054 (m), 912 (m), 839 (m), 732 (m), 704 (m), 535 (w) cm^{-1}. UV-vis (CH$_2$Cl$_2$): λ_{max} (ε) 590 nm (5,900 M^{-1} cm^{-1}), 429 nm (sh, 14,000 M^{-1} cm^{-1}), 391 nm (29,300 M^{-1} cm^{-1}), 274 nm (54,300 M^{-1} cm^{-1}). Mass Spec.

(ESI, +ve mode) m/z: $[M]^+$ calc'd for $[C_{55}H_{57}N_7NiO_4]^+$, 937.3825; found, 937.3853; difference: +2.8 ppm.

Representative synthesis of polymer 14

A grease-free Schlenk flask was charged with monomer **endo-13** (0.100 g, 0.117 mmol) before dry and degassed CH_2Cl_2 (4 mL) was added. Once the monomer was dissolved a 10.4 mg mL^{-1} CH_2Cl_2 solution of Grubbs' 3rd generation catalyst (0.20 mL, 2.34×10^{-3} mmol) was rapidly added in one portion. The polymerization proceeded for 3 h at 21 °C before it was terminated with ethyl vinyl ether (0.28 mL, 2.93 mmol) and stirred for an additional 30 min. The crude mixture was filtered through a short neutral alumina column (4 cm × 2.5 cm, CH_2Cl_2 then THF) before the solvent was removed *in vacuo*. The resultant polymer, a green solid was dissolved in THF (10 mL) and precipitated thrice into Et_2O (90, 90, and 15 mL) to afford polymer **14** as a green powder. Yield = 0.084 g, 84%. ^1H NMR (599.3 MHz, $CDCl_3$): δ 8.38–7.89 (m, 7H, aryl C*H* and triazole C*H*), 7.36 (br s, 2H, aryl C*H*), 6.63 (br s, 4H, aryl C*H*), 6.57 (br s, 4H, aryl C*H*), 5.63−5.06 (m, 2H, C=C*H*), 4.56 (br s, 2H, C*H*$_2$), 4.13 (br s, 2H, C*H*$_2$), 3.17 (br s, 1H, C*H*), 2.90 (m, 2H, C*H*$_2$), 2.70 (br s, 2H, C*H*$_2$), 2.50 (br s, 1H, C*H*), 2.33 (br s, 2H, C*H*$_2$), 2.17–1.75 (br s, 12H, macrocycle C*H*$_3$), 1.66 (br s, 2H, C*H*$_2$), 1.52−1.13 (m, 9H, C*H*$_2$), 0.88 (br s, 3H, C*H*$_3$). FT-IR (ATR): 3062 (w), 2928 (w), 2856 (w), 1728 (m), 1652 (m), 1604 (m), 1532 (s), 1450 (m), 1429 (m), 1375 (s), 1326 (m), 1224 (s), 1172 (s), 1054 (m), 911 (m), 859 (w), 727 (s) cm^{-1}. UV-vis (CH_2Cl_2): λ_{max} (ε) 592 nm (4,000 M^{-1} cm^{-1}), 430 nm (sh, 9,600 M^{-1} cm^{-1}), 391 nm (19,800 M^{-1} cm^{-1}), 274 nm (36,900 M^{-1} cm^{-1}). GPC (THF, conventional calibration): M_n = 24,100 g mol^{-1}, M_w = 26,500 g mol^{-1}, $Đ$ = 1.12).

Variation of Feed Molar Ratio: Using 0.05 g of monomer **endo-13** each, a series of five reactions were carried out according to the procedure described above. The catalyst molar feed

stock ratios (monomer:catalyst) were: 20, 40, 60, 80, and 100. The polymerization times were held constant at 90 min. The number average degree of polymerization (DP_n) for each sample was measured by GPC analysis using conventional calibration relative to polystyrene standards.

Monitoring Polymerization Progress with Timed Aliquots: A 1 mg mL^{-1} CH_2Cl_2 solution of 3-bromopyridine derivative of Grubbs' 3rd generation catalyst (1.0 mL, 6.4×10^{-3} mmol) was rapidly added in one portion to a 27 mg mL^{-1} CH_2Cl_2 solution of monomer ***endo*-13** (11 mL, 0.32 mmol) and the mixture was stirred at 21 °C. Eight samples were removed at different time intervals (60, 120, 210, 300, 450, 600, 750, and 900 s) and added into separate reaction flasks containing excess ethyl vinyl ether to terminate the polymerization. The number average molecular weights (M_n) were measured by GPC analysis using conventional calibration relative to polystyrene standards and monomer to polymer ratios were monitored using NMR analysis.

References

1 W.-Y. Wong and P. D. Harvey, *Macromol. Rapid Commun.*, 2010, **31**, 671−713.

2 G. R. Whittell, M. D. Hager, U. S. Schubert and I. Manners, *Nat. Mater.*, 2011, **10**, 176−188.

3 C. Friebe, M. D. Hager, A. Winter and U. S. Schubert, *Adv. Mater.*, 2012, **24**, 332−345.

4　H. Gu, R. Ciganda, S. Gatard, F. Lu, P. Zhao, J. Ruiz and D. Astruc, *J. Organomet. Chem.*, 2016, **813**, 95−102.

5　Y. Yan, J. Zhang, L. Ren and C. Tang, *Chem. Soc. Rev.*, 2016, **45**, 5232−5263.

6　R. L. N. Hailes, A. M. Oliver, J. Gwyther, G. R. Whittell and I. Manners, *Chem. Soc. Rev.*, 2016, **45**, 5358−5407.

7　T. J. O'Sullivan, B. Djukic, P. A. Dube and M. T. Lemaire, *Chem. Commun.*, 2009, 1903−1905.

8　M. Mazurowski, M. Gallei, J. Li, H. Didzoleit, B. Stühn and M. Rehahn, *Macromolecules*, 2012, **45**, 8970−8981.

9　Y. Zha, H. D. Thaker, R. R. Maddikeri, S. P. Gido, M. T. Tuominen and G. N. Tew, *J. Am. Chem. Soc.*, 2012, **134**, 14534−14541.

10　Q. Dong, G. Li, C.-L. Ho, M. Faisal, C.-W. Leung, P. W.-T. Pong, K. Liu, B.-Z. Tang, I. Manners and W.-Y. Wong, *Adv. Mater.*, 2012, **24**, 1034−1040.

11　C. Friebe, H. Görls, M. Jäger and U. S. Schubert, *Eur. J. Inorg. Chem.*, 2013, 4191−4202.

12　M. Erhard, K. Lam, M. Haddow, G. R. Whittell, W. E. Geiger and I. Manners, *Polym. Chem.*, 2014, **5**, 1264−1274.

13　S. Pandey, P. Lönnecke and E. Hey-Hawkins, *Eur. J. Inorg. Chem.*, 2014, 2456−2465.

14　A. Rabiee Kenaree, B. M. Berven, P. J. Ragogna and J. B. Gilroy, *Chem. Commun.*, 2014, **50**, 10714−10717.

15　M. Hadadpour, J. Gwyther, I. Manners and P. J. Ragogna, *Chem. Mater.*, 2015, **27**, 3430−3440.

16　H. Gu, R. Ciganda, P. Castel, J. Ruiz and D. Astruc, *Macromolecules*, 2016, **49**, 4763−4773.

17 B. Jiang, W. L. Hom, X. Chen, P. Yu, L. C. Payelka, K. Kisslinger, J. B. Parise, S. R. Bhatia and R. B. Grubbs, *J. Am. Chem. Soc.*, 2016, **138**, 4616−4625.

18 P. Yang, P. Pageni, M. P. Kabir, T. Zhu and C. Tang, *ACS Macro Lett.*, 2016, **5**, 1293−1300.

19 R. H. Staff, M. Gallei, M. Mazurowski, M. Rehahn, R. Berger, K. Landfester and D. Crespy, *ACS Nano*, 2012, **6**, 9042−9049.

20 J. Zhang, Y. P. Chen, K. P. Miller, M. S. Ganewatta, M. Bam, Y. Yan, M. Nagarkatti, A. W. Decho and C. Tang, *J. Am. Chem. Soc.*, 2014, **136**, 4873−4876.

21 A. Rabiee Kenaree and J. B. Gilroy, *Dalton Trans.*, 2016, **45**, 18229−18240.

22 Z. M. Al-Badri, R. R. Maddikeri, Y. Zha, H. D. Thaker, P. Dobriyal, R. Shunmugam, T. P. Russell and G. N. Tew, *Nat. Commun.*, 2011, **2**, 482.

23 L. Ren, J. Zhang, C. G. Hardy, S. Ma and C. Tang, *Macromol. Rapid Commun.*, 2012, **33**, 510−516.

24 S. Baljak, A. D. Russell, S. C. Binding, M. F. Haddow, D. O'Hare and I. Manners, *J. Am. Chem. Soc.*, 2014, **136**, 5864−5867.

25   H. Fukumoto, K. Yamane, Y. Kase and T. Yamamoto, *Macromolecules*, 2010, **43**, 10366−10375.

26 N. Novoa, J. P. Soto, R. Henríquez, C. Manzur, D. Carrillo and J.-R. Hamon, *J. Inorg. Organomet. Polym. Mater.*, 2013, **23**, 1247−1254.

27 E. Scamporrino and D. Vitalini, *Macromolecules*, 1992, **25**, 1625−1632.

28 M. T. Nguyen, R. A. Jones and B. J. Holliday, *Macromolecules*, 2017, **50**, 872−883.

29 V. L. Goedken, M. C. Weiss, D. Place and J. Dabrowiak, in *Inorg. Synth.*, ed. D. H. Busch, John Wiley & Sons, Inc., Hoboken, NJ, USA., 2007, ch. 30, pp. 115−119.

30 J. H. Niewahner, K. A. Walters and A. Wagner, *J. Chem. Educ.*, 2007, **84**, 477.

31 C. L. Bailey, R. D. Bereman, D. P. Rillema and R. Nowak, *Inorg. Chem.*, 1986, **25**, 933−938.

32 D. Kim, E. Kim, J. Byun, J. Choi, H. Na and Y. Park, *J. Coord. Chem.*, 2002, **55**, 505−516.

33 J. A. Paquette, E. R. Sauvé and J. B. Gilroy, *Macromol. Rapid Commun.*, 2015, **36**, 621−626.

34 J. A. Paquette and J. B. Gilroy, *J. Polym. Sci., Part A: Polym. Chem.*, 2016, **54**, 3257−3266.

35 F. A. Cotton and J. Czuchajowska, *Polyhedron*, 1990, **9**, 2553−2566.

36 P. Mountford, *Chem. Soc. Rev.*, 1998, **27**, 105−115.

37 C. L. Raston, P. J. Nichols and K. Baranyai, *Angew. Chem. Int. Ed.*, 2000, **39**, 1842−1845.

38 E. V. Basiuk, E. V. Rybak-Akimova, V. A. Basiuk, D. Acosta-Najarro and J. M. Saniger, *Nano Lett.*, 2002, **2**, 1249−1252.

39 S.-J. Liu, *Electrochim. Acta*, 2004, **49**, 3235−3241.

40 U. J. Williams, B. D. Mahoney, P. T. DeGregorio, P. J. Carroll, E. Nakamaru-Ogiso, J. M. Kikkawa and E. J. Schelter, *Chem. Commun.*, 2012, **48**, 5593−5595.

41 E. V. Basiuk, M. Martinez-Herrera, E. Álvarez-Zauco, L. V. Henao-Holguín, I. Puente-Lee and V. A. Basiuk, *Dalton Trans.*, 2014, **43**, 7413−7428.

42 A. Deronzier and M. J. Marques, *J. Electroanal. Chem.*, 1989, **265**, 341−353.

43 A. Deronzier and M. J. Marques, *J. Electroanal. Chem.*, 1992, **334**, 247−261.

44 H.-H. Huang, C.-G. Chao, S.-L. Lee, H.-J. Wu, C.-H. Chen and T.-Y. Luh, *Org. Biomol. Chem.*, 2012, **10**, 5948−5953.

45 B. Neises and W. Steglich, *Angew. Chem. Int. Ed.*, 1978, **17**, 522−524.

46 J. A. Berson and D. A. Ben-Efraim, *J. Am. Chem. Soc.*, 1959, **81**, 4083−4087.

47 R. H. Grubbs, A. G. Wenzel, D. J. O'Leary, and E. Khosravi, Handbook of Metathesis, Wiley-VCH Verlag GmbH & Co. KGaA, Weinheim, Germany, 2015.

48 C. W. Bielawski and R. H. Grubbs, *Prog. Polym. Sci.*, 2007, **32**, 1−29.

49 C. L. Bailey, R. D. Bereman, D. P. Rillema and R. Nowak, *Inorg. Chem.*, 1984, **23**, 3956−3960.

50 H. G. Na, D. C. Lee, J. W. Lim, J. H. Choi, J. C. Byun and Y. C. Park, *Polyhedron*, 2002, **21**, 917−923.

51 J. Gwyther, J. B. Gilroy, P. A. Rupar, D. J. Lunn, E. Kynaston, S. K. Patra, G. R. Whittell, M. A. Winnik and I. Manners, *Chem. Eur. J.*, 2013, **19**, 9186−9197.

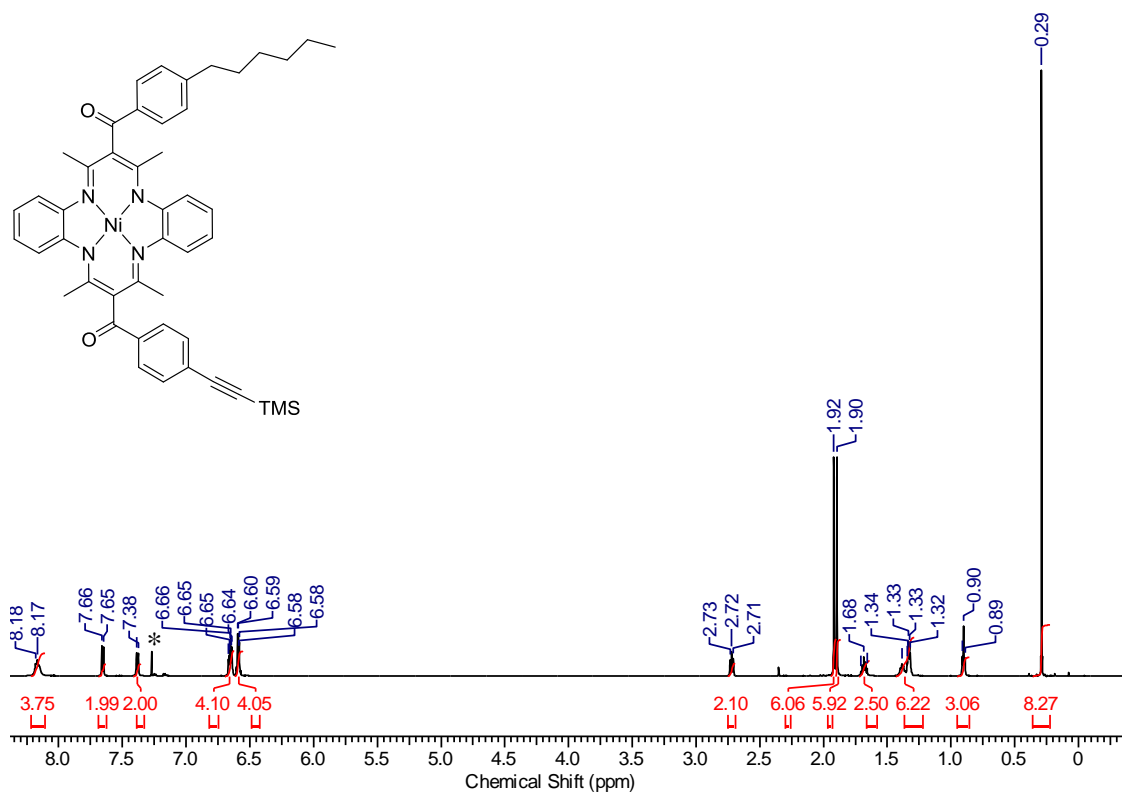52 M. Bertoldo, G. Zampano, F. L. Terra, V. Villari and V. Castelvetro, *Biomacromolecules*, 2011, **12**, 388−398.

Supplementary Information

Metal-containing polymers bearing pendant nickel(II) complexes of Goedken's macrocycle

Joseph A. Paquette, Amir Rabiee Kenaree and Joe B. Gilroy*

Department of Chemistry and the Centre for Advanced Materials and Biomaterials Research (CAMBR), The University of Western Ontario, 1151 Richmond St. N., London, Ontario, Canada, N6A 5B7. Tel: +1-519-661-2111 ext. 81561; E-mail: joe.gilroy@uwo.ca

Fig. S1 ^{1}H NMR spectrum of compound **9** in CDCl$_3$. Asterisks denote residual CHCl$_3$ and grease.

Fig. S2 ^{13}C{^{1}H} NMR spectrum of **9** in CDCl$_3$. Asterisks denote CDCl$_3$ and grease.

Fig. S3 ^{1}H NMR spectrum of compound **10** in CDCl$_3$. Asterisk denotes residual CHCl$_3$.
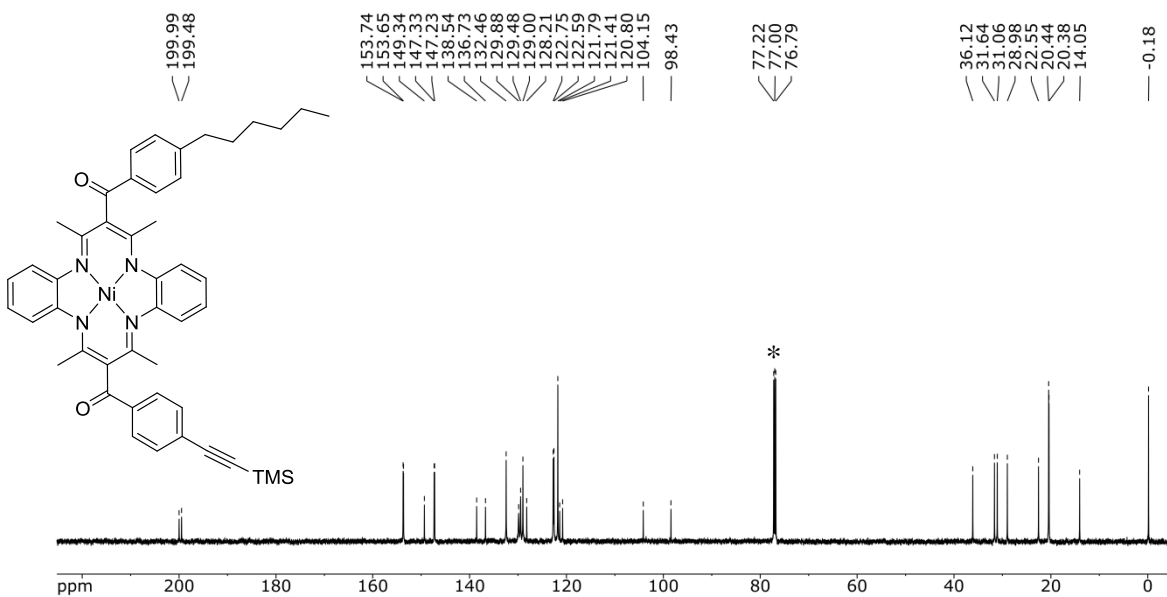
Fig. S4 ^{13}C{^{1}H} NMR spectrum of **10** in CDCl$_3$. Asterisk denotes CDCl$_3$.
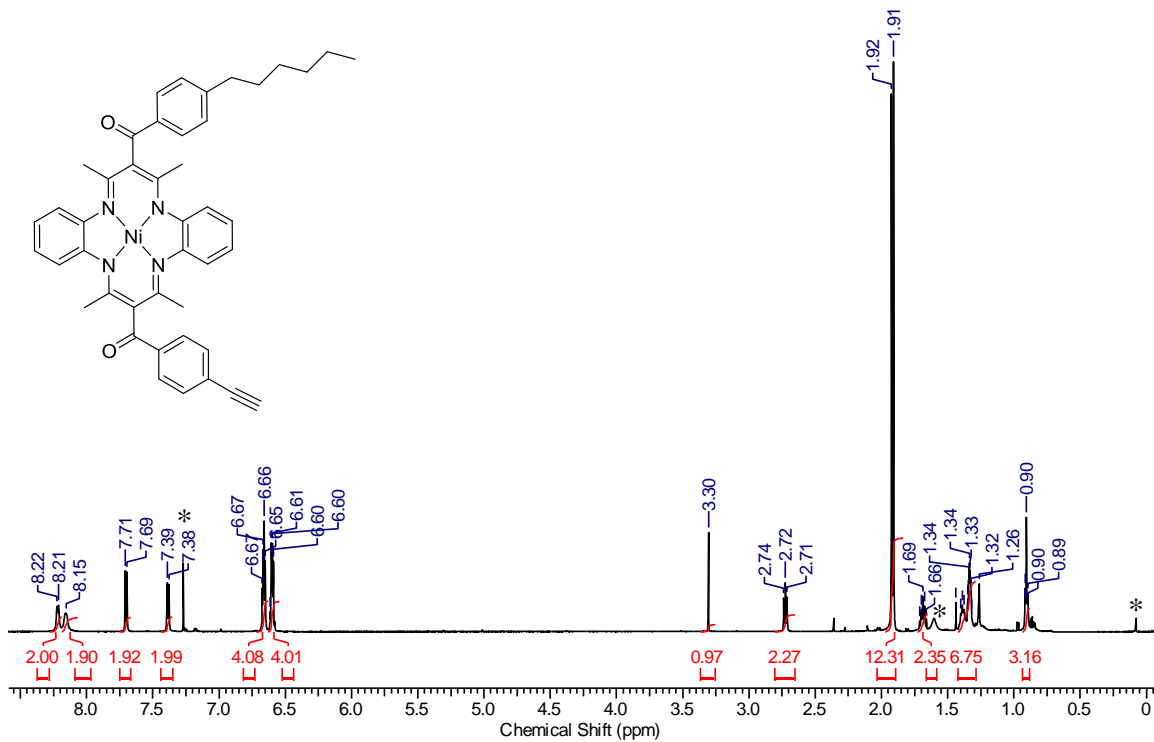
Fig. S5 ^{1}H NMR spectrum of compound **11** in CDCl$_3$. Asterisks denote residual CHCl$_3$, H$_2$O, and grease.
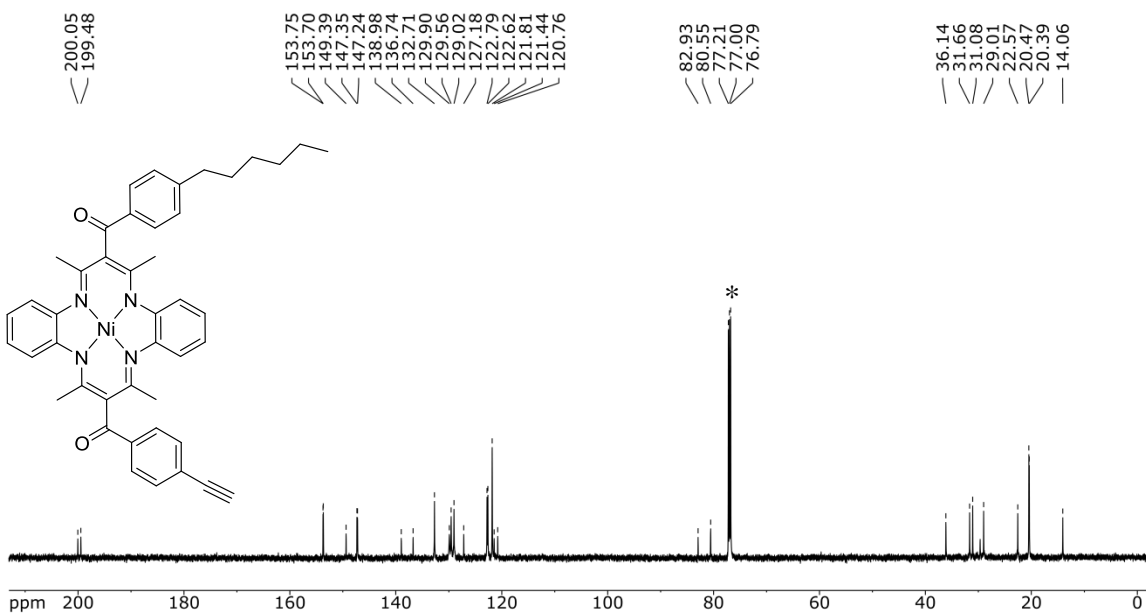
Fig. S6 ^{13}C{^{1}H} NMR spectrum of **11** in CDCl$_3$. Asterisk denotes CDCl$_3$.
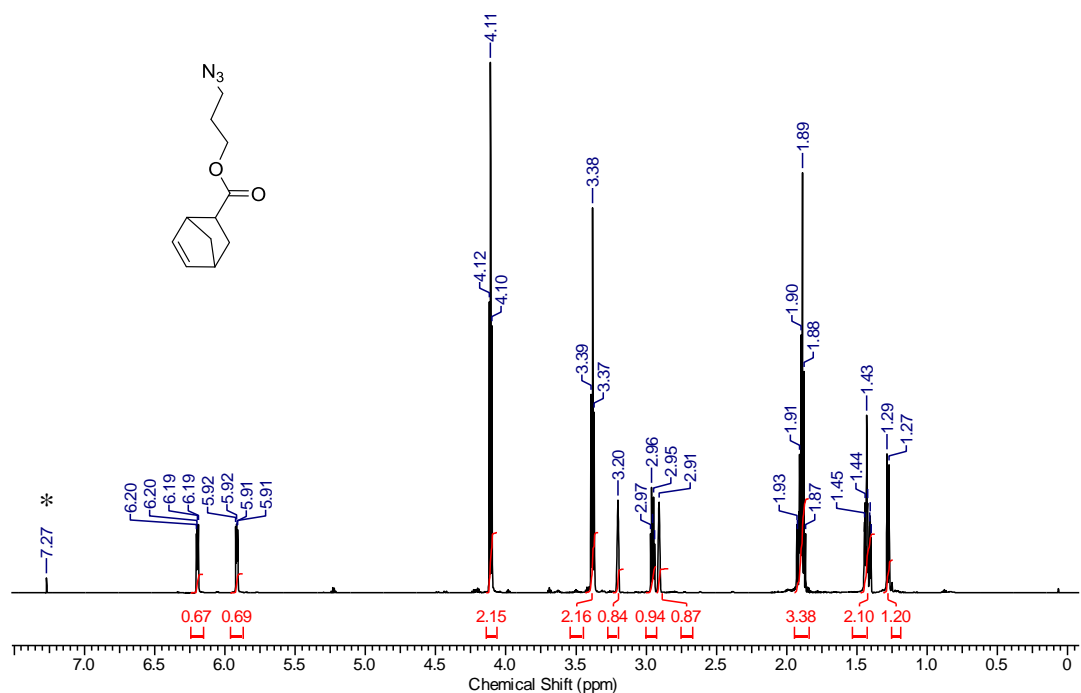
Fig. S7 ^{1}H NMR spectrum of compound ***endo*-12** in CDCl$_3$. Asterisk denotes residual CHCl$_3$.
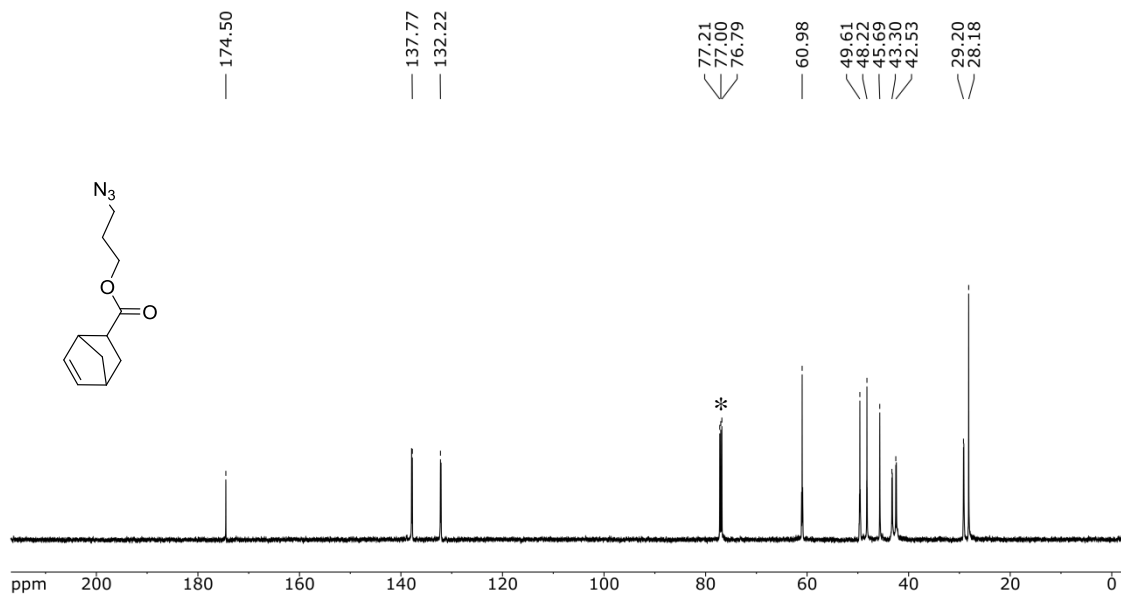
Fig. S8 ^{13}C{^{1}H} NMR spectrum of ***endo*-12** in CDCl$_3$. Asterisk denotes CDCl$_3$.
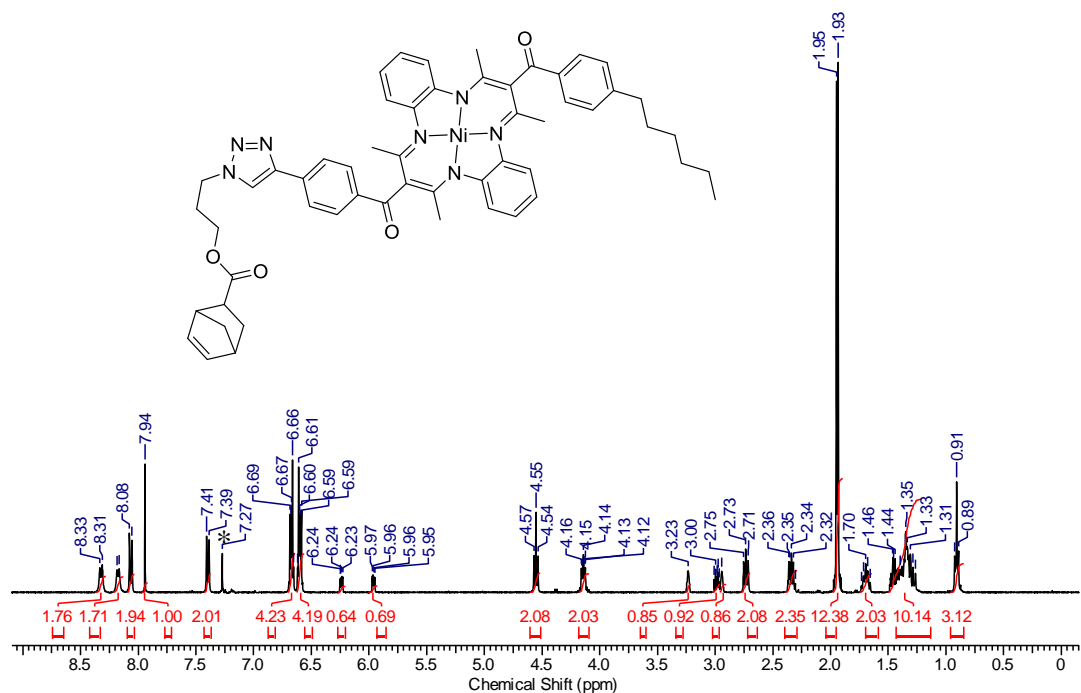
Fig. S9 ^{1}H NMR spectrum of compound *endo*-**13** in CDCl$_3$. Asterisk denotes residual CHCl$_3$.
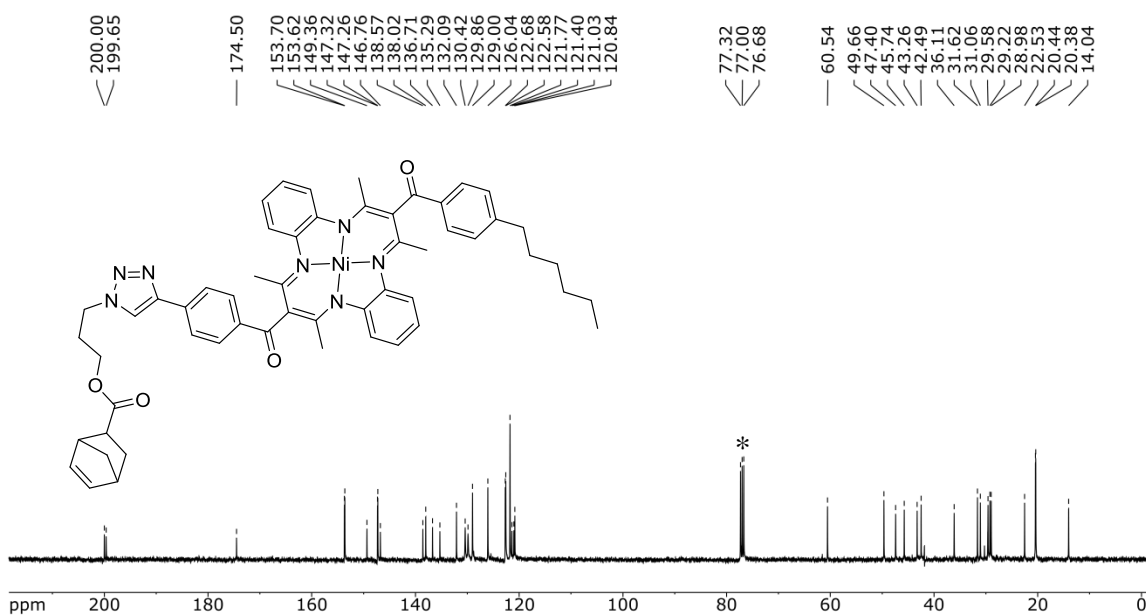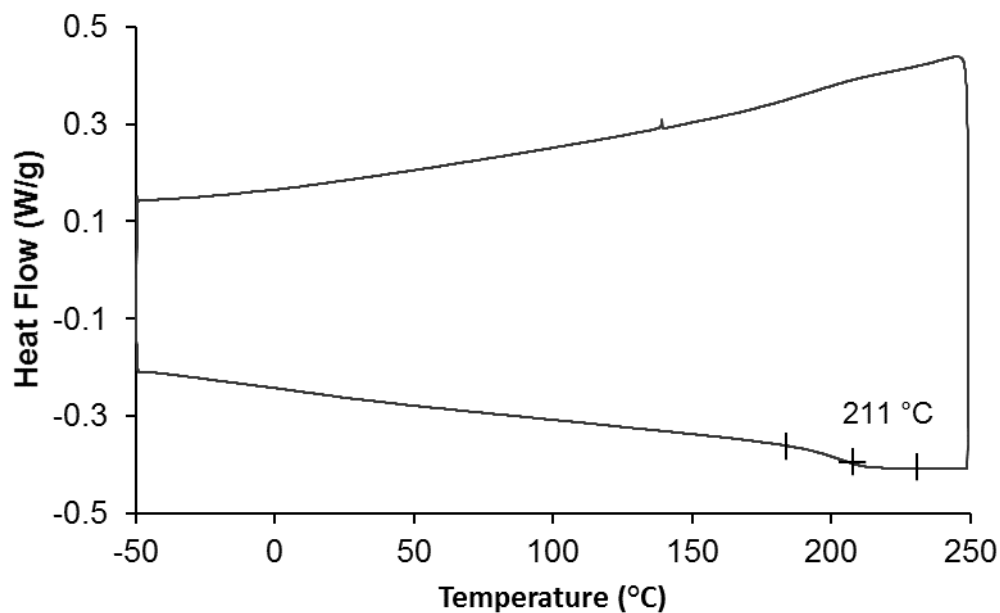

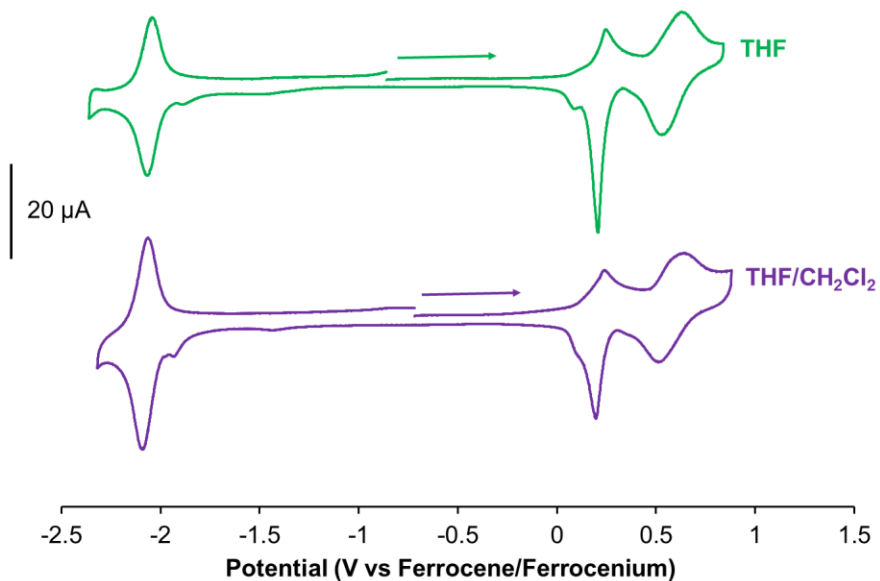**Fig. S10** ^{13}C{^{1}H} NMR spectrum of *endo*-**13** in CDCl$_3$. Asterisk denotes CDCl$_3$.
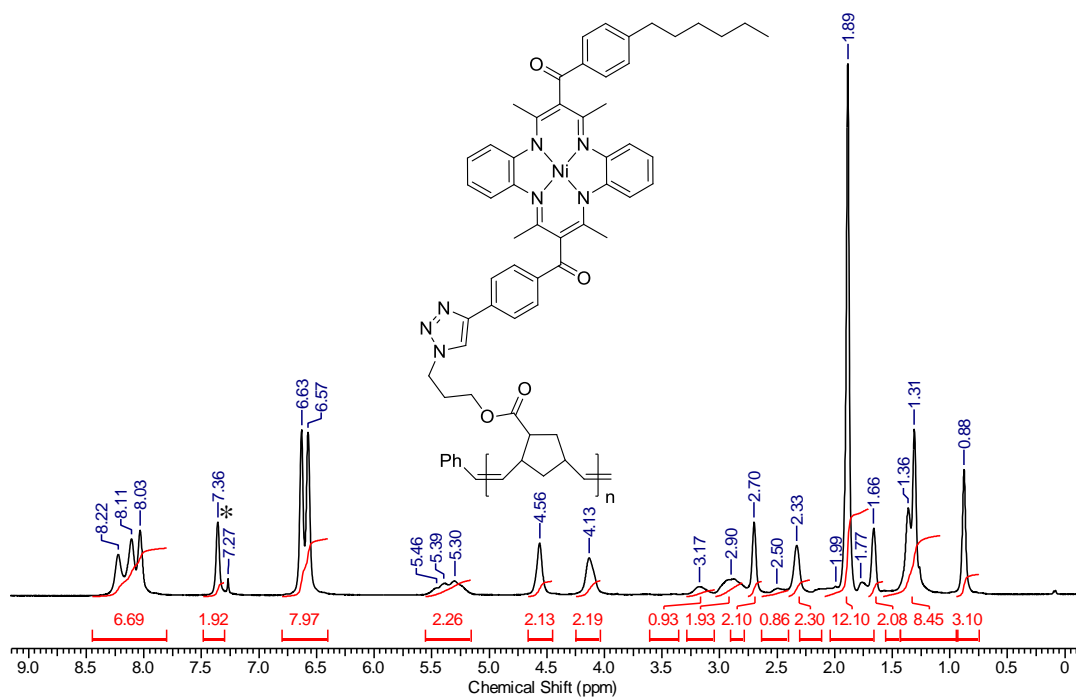
Fig. S11 Representative ^{1}H NMR spectrum of polymer **14** in CDCl₃. Asterisk denotes residual CHCl₃.
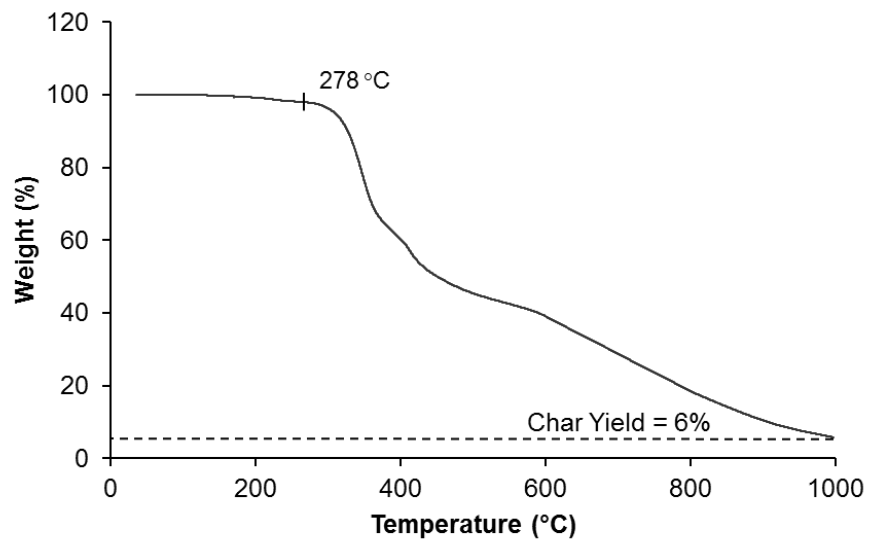
Fig. S12 TGA trace for polymer **14**.

Fig. S13 DSC thermogram of polymer **14**. The data presented are from the second heating/cooling cycle.

Fig. S14 Cyclic voltammograms of polymer **14** recorded at a scan rate of 250 mV s^{-1} in THF (green) and THF/CH$_2$Cl$_2$ (1/1) (purple) solutions containing 1×10^{-3} M analyte and 0.1 M [nBu$_4$N][PF$_6$] as supporting electrolyte.